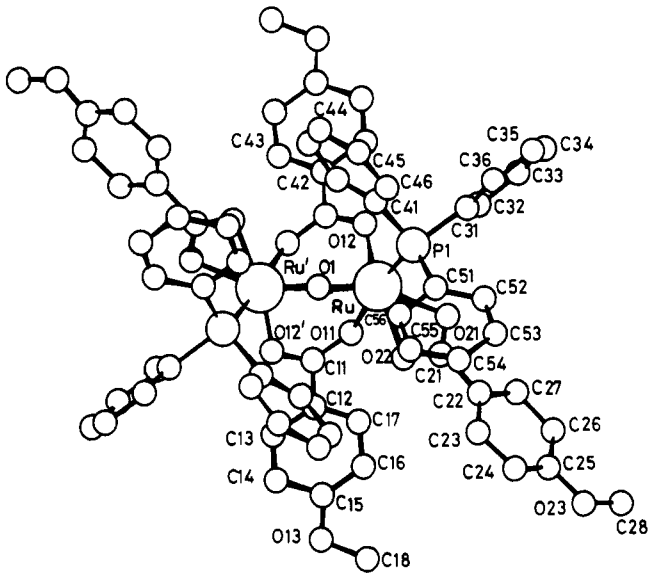

Figure 6. Perspective view of $Ru_2O(O_2CC_6H_4\text{-}p\text{-}OMe)_4(PPh_3)_2$ (**2b**) along with the atom-labeling scheme.

in **1a** and **2b**, are similar to the M–M distances known[5] in complexes with an $\{M_2(\mu\text{-}O)(\mu\text{-}O_2CR)_2^{2+}\}$ core. The Ru–O–Ru angles in **1a** and **2b** are near 120°. The important structural parameters in these compounds are (i) the Ru–Ru distance and (ii) the Ru–O–Ru angle. Table VI lists the available data on diruthenium compounds.[5,6] The Ru–Ru interaction is expected to be dependent on the two above-cited parameters. The smaller Ru–O–Ru angle is expected to shorten the Ru–Ru distance. The data presented in Table VI show that the compound **2b** has the shortest Ru–Ru distance and the smallest Ru–O–Ru angle. The distance is still much longer than the Ru–Ru single bond distances known in the following edge-sharing bioctahedral diruthenium(III) compounds with a $\sigma^2\pi^4\pi^{*4}$ configuration: $Ru_2Cl_6(dmpm)_2$, 2.933 (1) Å;[33] $Ru_2(ap)_6(PMe_2Ph)_2$, 2.573 (2) Å;[32] $Ru_2(Ph)_2(PhCONH)_2[Ph_2POC(Ph)N]_2$, 2.566 (1) Å[28] (Hap = 2-aminopyridine). The formation of a direct Ru–Ru bond in **1** and **2** seems to be unlikely. The diamagnetic nature of **1** and **2** is, possibly, due to the coupling of the two t_{2g}^5 Ru(III) centers through the oxo bridge, as is proposed[20] for related oxo-bridged triruthenium systems. The diosmium(IV) compounds $Os_2O(O_2CR)_2(PPh_3)_2Cl_4$, are also known[15] to be diamagnetic with an Os–Os separation of 3.440 Å. Structural data on these systems containing the $\{Ru_2(\mu\text{-}O)(\mu\text{-}O_2CR)_2^{2+}\}$ core strongly suggest[38] that the intense colors of these compounds are due to charge-transfer transitions involving the $\{Ru_2(\mu\text{-}O)^{4+}\}$ unit held by two carboxylato bridges.

Acknowledgment. We are grateful to the Council of Scientific and Industrial Research, New Delhi, for financial support. We thank Professor H. Manohar and I. I. Mathews for their help in the structural studies.

Supplementary Material Available: For $Ru_2O(O_2CPh)_2(MeCN)_4(PPh_3)_2(ClO_4)_2\cdot H_2O$ (**1a**) and $Ru_2O(O_2CC_6H_4\text{-}p\text{-}OMe)_4(PPh_3)_2$ (**2b**), tables of thermal parameters and bond lengths and angles (10 pages); tables of observed and calculated structure factors (39 pages). Ordering information is given on any current masthead page.

(38) A recent report by Neubold et al. (ref 5) has shown that protonation of the μ-oxo bridge has a profound effect on the magnetic and electronic properties of the diruthenium(III) compounds. After submission of this manuscript, an article on similar types of diruthenium(III) compounds containing tris(1-pyrazolyl)methane facial ligands is reported: Llobet, A.; Curry, M. E.; Evans, H. T.; Meyer, T. J. *Inorg. Chem.* **1989**, *28*, 3131.

Contribution from the Department of Chemistry, University of Illinois at Chicago, Chicago, Illinois 60680

Molecular Architecture of a Novel Vertex-Sharing Biicosahedral Cluster $[(p\text{-}Tol_3P)_{10}Au_{13}Ag_{12}Br_8](PF_6)$ Containing a Staggered–Staggered–Staggered Configuration for the 25-Atom Metal Framework

Boon K. Teo,* Hong Zhang, and Xiaobo Shi

Received May 24, 1989

The crystal and molecular structure of a 25-atom metal cluster, $[(p\text{-}Tol_3P)_{10}Au_{13}Ag_{12}Br_8]^+(PF_6)^-$ (**1**), has been determined by single-crystal X-ray crystallography. The complex $[(p\text{-}Tol_3P)_{10}Au_{13}Ag_{12}Br_8](PF_6)\cdot 10EtOH$ crystallizes in a unit cell of triclinic $P\bar{1}$ symmetry with lattice parameters a = 16.971 (2) Å, b = 17.431 (2) Å, c = 21.825 (2) Å, α = 78.20 (6)°, β = 72.33 (6)°, γ = 72.13 (4)°, and Z = 1. The structure was refined to R_1 = 9.8%, R_2 = 11.6% for 9150 independent reflections with $I > 3\sigma(I)$. The metal framework of **1** can be described as two 13-atom centered icosahedra sharing a common vertex. As such, it belongs to a novel series of high-nuclearity Au–Ag clusters whose structures are based on vertex-sharing (centered) icosahedra. The structural systematics of this new class of supraclusters led to the concept of "cluster of clusters", which is useful in the design, preparation, and characterization of large metal clusters of increasingly high nuclearity via vertex-, edge-, and face-sharing and/or close packing of smaller cluster units as building blocks.

(I) Introduction

A cluster is an aggregate of atoms or molecules. Current interest in clusters stems from the fact that the collective behavior of a cluster often differs significantly from that of its constituents.

Chemists have been able to prepare and/or observe a wide variety of clusters in gas, liquid, solution, or solid phases. Some clusters are naked (for example, Bi_8^{2+} [1a] and Ge_9^{2-} [1b]), while others are ligated with ligands such as phosphines (e.g., $[Au_{13}Cl_2(PMe_2Ph)_{10}]^{3+}$ [2]) and carbonyls (e.g., $[Pt_{19}(CO)_{22}]^{4-}$ [3]). They can either be discrete clusters in solution or extended clusters in solid states. Finally, atoms (or molecules) within a cluster can be held together by ionic, covalent, metallic, or hydrogen bonding,

(1) (a) Krebs, B.; Hucke, M.; Brendel, C. S. *Angew. Chem., Int. Ed. Engl.* **1982**, *21*, 445. (b) Belin, C. H. E.; Corbett, J. D.; Cisar, A. *J. Am. Chem. Soc.* **1977**, *99*, 7163.

(2) Briant, C. E.; Theobold, B. R. C.; White, J. W.; Bell, L. K.; Mingos, D. M. P.; Welch, A. J. *J. Chem. Soc., Chem. Commun.* **1981**, 201.

(3) Washecheck, D. M.; Wucherer, E. J.; Dahl, L. F.; Ceriotti, A.; Longoni, G.; Manassero, M.; Sansoni, M.; Chini, P. *J. Am. Chem. Soc.* **1979**, *101*, 6110.

0020-1669/90/1329-2083$02.50/0

as well as weak van der Waals interactions.

A metal cluster, as defined by Cotton,[4] is "a group of two or more metal atoms in which there are substantial and direct bonds between the metal atoms". Large metal clusters[5,6] (containing, for example, dozens of metal atoms) are of particular interest in that they lie in the region of aggregation between individual atoms and bulk metal. Investigations of the chemical and physical properties of these clusters will therefore shed light on how, where, and when metallic behavior begins or ends. In other words, how many metal atoms must a cluster have before it begins to behave as a metal? Conversely, how small must metal particles become before they lose their metallic character? In the region between one and a large number of associated atoms, there is, evidently, some intermediate number or numbers that determine the presence or absence of metallic or other bulk properties (though the transition may well be a gradual, rather than an abrupt, process).

A crucial first step toward such a goal is the preparation and structural characterization of large, structurally well-defined metal clusters with discrete size and shape approaching that of small metal particles.

Recent developments in cluster synthesis[7-9] have produced high-nuclearity metal *clusters* approaching small *crystallites* in *size* and *shape*. For example, metal carbonyl clusters containing a few dozen atoms, $[Pt_{38}(CO)_{44}H_2]^{2-}$,[5a] $[Rh_{22}(CO)_{37}]^{4-}$,[5b] $[Rh_{22}(CO)_{35}H_{5-q+x}]^{q-}$ (q = 4, 5),[5c] $[Ni_{12}(CO)_{21}H_{4-n}]^{n-}$ (n = 2, 3, 4),[5d] $[Os_{10}C(CO)_{24}]^{2-}$,[5e] and $[Ru_{10}C_2(CO)_{24}]^{2-}$,[5f] have been synthesized and characterized structurally. Also worth mentioning are the following large mixed-metal clusters: $[Pt_6Ni_{38}(CO)_{48}H_{6-n}]^{n-}$, ($n$ = 4, 5),[6a] $[Fe_6Pd_6(CO)_{24}H]^{3-}$,[6b] and $[Pt_nRh_{13-n}(CO)_{24}]^{(5-n)-}$ (n = 1, 2).[6c] Homonuclear or mixed-metal clusters may also be referred to as *metal alloy clusters*. Many of these discrete clusters can be considered as fragments of the metallic lattice. As such, they can also be considered as a small chunk of metal or a small metal particle.

This paper reports in detail the single-crystal X-ray structure of a novel 25-atom cluster containing 13 Au and 12 Ag atoms: $[(p\text{-}Tol_3P)_{10}Au_{13}Ag_{12}Br_8]^+$ as a PF_6^- salt (**1**). The metal framework of the title compound **1** can be described as two 13-atom centered icosahedra sharing a common vertex. As such, it belongs to a novel series of high-nuclearity Au–Ag clusters whose structures are based on vertex-sharing (centered) icosahedra. The structural systematics of this new class of supraclusters led to the concept of "cluster of clusters", which can be useful in the design, preparation, and characterization of high-nuclearity supraclusters via vertex-, edge-, and face-sharing and/or close-packing of smaller cluster units as building blocks.[10,11]

Table I. Summary of Crystal Data, Collection and Reduction of X-ray Diffraction Data, and Solution and Refinement of Structure of $[(p\text{-}Tol_3P)_{10}Au_{13}Ag_{12}Br_8](PF_6)\cdot 10EtOH$ (**1**)

A. Crystal Data	
formula	$[(p\text{-}Tol_3P)_{10}Au_{13}Ag_{12}Br_8](PF_6)\cdot 10EtOH$
cryst color	dark red
cryst shape	prism
cryst size, mm³	0.1 × 0.08 × 0.1
cell params (errors)	
a, Å	16.971 (2)
b, Å	17.431 (2)
c, Å	21.825 (2)
α, deg	78.20 (6)
β, deg	72.33 (6)
γ, deg	72.13 (4)
V, Å³	5810.7 (4)
Z	1
Laue sym	triclinic
space group	$P\bar{1}$
system absences	no conditions
equiv posns	$-x, -y, -z$
B. Collection and Reduction of X-ray Diffraction Data	
diffractometer	Enraf-Nonius CAD4
radiation	Mo Kα
wavelength, Å	0.7107
temp, °C	23 ± 2
scan technique	$\omega/2\theta$
scan rate (limits), deg/min	4–16
scan range, deg	0.6 + 0.35 tan θ
no./freq of std reflcns	3/200
2θ limits, deg	$2 < 2\theta < 46$
cut off of obsd data	$3\sigma(I)$
unique data[a]	9150
octants	$\pm h, \pm k, +l$
linear abs coeff	109.8
abs cor	ψ scan
range of transm	81.0%–99.2%
C. Solution and Refinement of Structure	
technique of soln	direct methods
method of refinement	full-matrix least squares[b]
std dev	full variance–covariance
isotropic converg[c]	R_1 = 13.6%, R_2 = 15.5%
isotropic–anisotropic converg	R_1 = 9.8%, R_2 = 11.6%
max shifts (Δ/σ)	1
data/params	9150/759
max resid intens of final diff map, e/Å³	1.0

[a] The raw intensity is given as I_{raw} = (20.116 × ATN) × (C – RB)/NPI, where C = total counts, R = ratio of scan time to background counting time, B = total background counts, NPI = ratio of fastest possible scan rate to scan rate for the measurement, and ATN = attenuator factor (10.7 for Mo in our case). The observed structure factor amplitude is obtained as the square root of the intensity after correction for Lorentz-polarization: $F_{obs} = (I_{raw}/L_p)^{1/2}$. [b] All least-squares refinements were based on the minimization of $\sum w_i||F_o| - |F_c||^2$ with the individual weights $w_i = 1/\sigma(F_o)^2$. Atomic scattering factors used for all atoms are from: Cormer, D. T.; Waber, J. T. *International Tables for X-ray Crystallography*; The Kynoch Press: Birmingham, England, 1974; Vol. IV, Table 2.2B. Cromer, D. T.; Mann, J. B. X-ray Scattering Factors Computed From Numerical Hartree-Fock Wave Functions. *Acta Crystallogr., Sect. A* **1968**, *A24*, 321–324. [c] $R_1 = [\sum||F_o| - |F_c||/\sum|F_o|] \times 100\%$ and $R_2 = [\sum w_i||F_o| - |F_c||^2/\sum w_i|F_o|^2]^{1/2} \times 100\%$. See supplementary material for a listing of observed and calculated structure factors.

(II) Experimental Section

A. Preparation and Crystallization of Compound 1. The title compound **1** was prepared by reducing a mixture (Au:Ag = 1:1) of $(p\text{-Tol})_3PAuBr$ (0.1 mmol) and $[(p\text{-}Tol_3P)AgBr]_4$[12] (0.025 mmol) in 100

(4) Cotton, F. A. *Q. Rev. Chem. Soc.* **1966**, *20*, 389.
(5) (a) Longoni, G.; Dahl, L. Unpublished results. (b) Martinengo, S.; Fumagalli, A.; Bonfichi, R.; Ciani, G.; Sironi, A. *J. Chem. Soc., Chem. Commun.* **1982**, 825. (c) Vidal, J. L.; Schoening, R. C.; Troup, J. M. *Inorg. Chem.* **1981**, *20*, 227. (d) Broach, R. W.; Dahl, L. F.; Longoni, G.; Chini, P.; Schulz, A. J.; Williams, J. M. *Adv. Chem. Ser.* **1978**, *No. 167*, 93. (e) Jackson, P. F.; Johnson, B. F. G.; Lewis, J.; Nelson, W. J. H.; McPartlin, M. *J. Chem. Soc., Dalton Trans.* **1982**, 2099. (f) Hayward, C. M. T.; Shapley, J. R.; Churchill, M. R.; Bueno, C.; Rheingold, A. L. *J. Am. Chem. Soc.* **1982**, *104*, 7347.
(6) (a) Ceriotti, A.; Demartin, F.; Longoni, G.; Manassero, M.; Marchionna, M.; Piva, G.; Sansoni, M. *Angew. Chem., Int. Ed. Engl.* **1985**, *24*, 697. (b) Longoni, G.; Manassero, M.; Sansoni, M. *J. Am. Chem. Soc.* **1980**, *102*, 3242. (c) Fumagalli, A.; Martinengo, S.; Ciani, G.; Sironi, A. *J. Chem. Soc., Chem. Commun.* **1983**, 453. (d) Boyle, P. D.; Johnson, B. J.; Buehler, A.; Pignolet, L. H. *Inorg. Chem* **1986**, *25*, 5. (e) Alexander, B. D.; Boyle, P. D.; Johnson, B. J.; Casalnuovo, A. L.; John, S. M.; Mueting, A. M.; Pignolet, L. H. *Inorg. Chem.* **1987**, *26*, 2547. (f) Steggerda, J. J.; Bour, J. J.; van der Velden, J. W. A. *Recl.: J. R. Neth. Chem. Soc.* **1982**, *101*, 164.
(7) Kharas, K.; Dahl, L. *Adv. Chem. Phys.* **1988**, *70* (2), 1.
(8) (a) Chini, P. *Gazz. Chim. Ital.* **1979**, *109*, 225. (b) Chini, P. *J. Organomet. Chem.* **1980**, *200*, 37. (c) Chini, P.; Longoni, G.; Albano, V. G. *Adv. Organomet. Chem.* **1976**, *14*, 285.
(9) Johnson, B. F. G., Ed. *Transition Metal Clusters*; Wiley-Interscience: Chichester, England, 1980.
(10) (a) Teo, B. K.; Hong, M. C.; Zhang, H.; Huang, D. B. *Angew. Chem., Int. Ed. Engl.* **1987**, *26*, 897. (b) Teo, B. K.; Hong, M.; Zhang, H.; Huang, D.; Shi, X. *J. Chem. Soc., Chem. Commun.* **1988**, 204. (c) Teo, B. K. *Polyhedron* **1988**, *7*, 2317.
(11) (a) Teo, B. K.; Zhang, H. *Inorg. Chem.* **1988**, *27*, 414. (b) Teo, B. K.; Zhang, H. *Inorg. Chim. Acta* **1988**, *144*, 173. (c) The G_7, S_7, B_7, T_7, and N_7 values of $s_7(75)$, the pentagonal-bipyramidal array of seven vertex-sharing icosahedra (cf. Figure 1f in ref 11a) should be 75, 67, 43 or 46, 445 or 448, and 890 or 896, respectively.[11a]
(12) Teo, B. K.; Calabrese, J. C. *Inorg. Chem.* **1976**, *15*, 2467.

mL of ethanol with $NaBH_4$ in 10 mL of absolute ethanol. The solution turned dark red immediately upon addition of the reducing agent. The mixture was allowed to react over a period of 24 h until the completion of the reaction. The solution was then filtered with a frit and washed several times with ethanol. To the filtrate was added a solution of 0.1 mmol of $NaPF_6$ in 20 mL of ethanol. The reaction mixture was allowed to stir for a few more minutes and then filtered. The title compound (**1**), in the form of dard-red prisms, was recrystallized from ethanol/hexane (ratio approximately 5:1) by evaporation at room temperature.

B. Collection and Reduction of X-ray Data. A dark red prismatic crystal of dimensions 0.1 mm × 0.08 mm × 0.1 mm was selected and sealed in a glass capillary with the mother liquor. Single-crystal X-ray diffraction data were collected on an Enraf-Nonius CAD4 diffractometer with use of graphite-monochromatized Mo Kα radiation (λ = 0.7107 Å). Unit cell parameters and the orientation matrix were obtained by least-squares analysis of the diffractometer setting angles of 25 well-centered reflections with $6° \le 2\theta \le 20°$. Details of the crystal parameters and data collection are summarized in Table I. Three standard reflections were monitored every 200 measurements over the entire period of data collection. The diffraction peaks were relatively weak and did not extend beyond $2\theta > 46°$. It yielded 9150 independent reflections with $I > 3\sigma(I)$. A decay correction was made on collected data. The observed intensities were corrected for Lorentz and polarization effects and for absorption (ψ scan). Extinction correction was made with least-squares refinements. The atomic and anomalous scattering factors used were those in the SDP package. The measured lattice parameters (25 °C) for the triclinic unit cell are a = 16.971 (2) Å, b = 17.431 (2) Å, c = 21.825 (2) Å, α = 78.20 (6)°, β = 72.33 (6)°, and γ = 72.13 (4)°; the unit cell volume equals 5810.7 (4) Å^3. The centrosymmetric space group $P\bar{1}$ was confirmed by successful solution and refinement of the structure. Since the center of the cluster (0,0,0) lies on a crystallographic center of symmetry, the analysis required the location of seven Au, six Ag, four Br, and five $(Tol)_3P$ groups in an asymmetric unit.

C. Solution and Refinement of the Structure. 1. Direct Methods Analysis and Fourier Syntheses. Initial positions of the metal atoms were obtained from direct methods, and the Br and P atoms were located via Fourier syntheses. The tolyl carbon atoms (viz., tolyl-ring carbons bonded to the phosphorus atoms P*i*: C*imj*, i = 1–5, j = 1–7, m = A–C) and the PF_6^- anion were revealed from subsequent difference Fourier syntheses. A few missing methyl carbon atoms (C7) of the tolyl groups were calculated by use of an idealized geometry (viz., an assumed C4–C7 distance of 1.47 Å and a linear C1···C4–C7 arrangement where the ring atoms are numbered C1–C6). Subsequent refinements of the metal core with all tolyl carbon atoms were successful, resulting in discrepancy factors of $R_1 = [\sum||F_o| - |F_c||/|F_o|] \times 100\% = 13.6\%$, $R_2 = [\sum w(|F_o| - |F_c|)^2/\sum w|F_o|^2]^{1/2} \times 100\% = 15.5\%$, where $w_i = 1/\sigma_i^2(F_o)$ for 9150 reflections with $I > 3\sigma(I)$.

2. Crystal-Disordered Anion and Solvent Molecules. The single crystallographically independent anion PF_6^- was revealed by successive difference Fourier synthesis and treated as position disordered with occupancy factor of $^1/_2$ (see section III.E for a detailed discussion). The least-squares refinements were successful with reasonable thermal parameters.

All solvent atoms, which were revealed by successive difference Fourier synthesis, are highly disordered. Therefore, the occupancy factors of the solvent atoms were first refined by using an isotropic thermal parameter of B = 8 Å^2 (roughly the average of the tolyl carbon atoms). The refined occupancy factors of these atoms were then fixed, and their thermal parameters (B's) were refined along with the positional and thermal parameters for all heavy atoms; all tolyl groups were included in the refinement as fixed-atom contributions. No hydrogen atoms were included in the refinement due to the large number of parameters involved.

3. Final Cycles of Refinement. In the final cycles of the refinement, anisotropic thermal parameters were used for the heavy atoms (Au, Ag, Br, P) and the anion atoms (P, F), while the tolyl atoms and the highly disordered solvent atoms were refined isotropically. Final $R_1 = [\sum||F_o| - |F_c||/|F_o|] \times 100\%$ and $R_2 = [\sum w(|F_o| - |F_c|)^2/\sum w|F_o|^2]^{1/2}$ values were 9.8% and 11.6%, respectively, for 9150 unique reflections with $I > 3\sigma(I)$. The final difference map showed no peaks greater than 1 e/Å^3 (except near heavy atoms). Final atomic coordinates and thermal parameters with estimated standard deviations are presented in Tables II and A (supplementary material), respectively. The tolyl carbon atoms are numbered as C*iAj*, C*iBj*, and C*iCj*, designating the *j*th carbon atom (j = 1–7) of rings A, B, and C bonded to the *i*th phosphine (i = 1–5), respectively. The positional and thermal parameters and the refined occupancy factors of solvent atoms are summarized in Table B of the supplementary material. Selected interatomic distances and bond angles together with the estimated standard deviations, calculated from the full inverse matrix, are given in Tables III and IV (see Tables C and D of the supplementary material for full listings), respectively. Observed and calculated structure factors are deposited as supplementary material. Least-squares calculations of "best" molecular planes formed by certain groups of atoms and the perpendicular distance of these and other atoms from those planes are summarized in Table E (supplementary material). Intra- and intermolecular interactions in cluster **1** are summarized in Table F (supplementary material).

(III) Discussions

A. Molecular Architecture. The molecular architecture of the $[P_{10}Au_{13}Ag_{12}Br_8]^+$ framework of the 25-atom cluster **1** is portrayed in Figure 1: (a) metal framework only; (b) with ligands; (c) with α-carbons of the tolyl groups. As pointed out by Teo and Keating in 1984 in the description of their 25-atom cluster,[13] there are several ways to describe the metal framework of the structure. The most obvious description of the metal framework is as two 13-atom (Au_7Ag_6) Au-centered icosahedra sharing one Au vertex. As such, the 13 Au atoms can be divided into two categories: 10 (two pentagonal Au_5 rings) on the surface and 3 in the interior. The 12 Ag atoms can be classified into two types: 10 on the peripherals (two pentagonal Ag_5 rings; see also Figure 2) and 2 on the idealized 5-fold axis.

The structure can also be considered as three interpenetrating icosahedra with three Au atoms completely encapsulated within the three icosahedral cages. Under $P\bar{1}$ space group, the molecule has a crystallographically imposed inversion center at Au13 (the prime symbol designates the symmetry-related atoms). As such, cluster **1** is situated at the origin of the unit cell.

It should be noted that there is an idealized 5-fold symmetry axis passing through atoms Ag11, Au11, Au13, Au11′, and Ag11′ such that the cluster can be viewed as having a metal arrangement of 1 (Ag):5 (Au):1 (Au):5 (Ag):1 (Au):5 (Ag):1 (Au):5 (Au):1 (Ag) where the number 5 represents a pentagonal ring.

There are 10 tri-*p*-tolylphosphine and 8 bromide ligands. The 10 tri-*p*-tolylphosphine ligands are coordinated to 10 peripheral (surface) Au atoms. Six bromide ligands connect the two central silver pentagons, as depicted in Figure 2 (viewed along the idealized 5-fold axis). Of these six bromide ligands, two, Br2 and Br2′, are doubly bridging, while the other four, Br1, Br3, Br1′, and Br3′, are asymmetric triply bridging. Two terminal bromide ligands, Br11 and Br11′, are bonded to the two Ag atoms on the idealized 5-fold axis.

Interatomic distances are tabulated in Table III. All metal–metal contacts, ranging from 2.711 (3) to 3.107 (4) Å, can be considered as more or less bonding distances. The metal–metal distances follow the approximate trend of Au–Au < Au–Ag < Ag–Ag.

B. Three Icosahedral Cages. In the interpenetrating triicosahedra description, the cluster **1** has two *outer* Au-centered Au_7Ag_6 icosahedra and one *inner* Au-centered Au_3Ag_{10} icosahedron. An icosahedral hole is capable of housing an additional "interior atom" of roughly 10% smaller in size than the "surface atoms". Thus, we find that the metal–metal distances involving the three centroids of the three icosahedra (Au11, Au13, Au11′) are among the shortest in cluster **1** (cf. Table III). For example, the 12 metal–metal distances around Au11 can be categorized into four groups: 2.738 Å to Ag11, 2.718 Å to the Au pentagon (Au1–Au5), 2.855 Å to the Ag pentagon (Ag1–Ag5), and 2.824 Å to Au13. Similarly, the 12 metal–metal distances around Au13 can be grouped into two types: 2.824 Å to Au11 and Au11′ and 2.867 Å to the Ag pentagons (Ag1–Ag5 and Ag1′–Ag5′).

There is, however, a significant difference between the three icosahedral centers. While Au11 and Au11′ each has an isotropic thermal parameter of 2 Å^2, which is somewhat smaller than that of the "surface" gold atoms (Au1–Au5 average: 3 Å^2), Au13 has a significantly higher value of 7 Å^2 (cf. section G).

An idealized icosahedron belongs to the I_h point group, which has an inversion symmetry. Therefore it should have six linear arrays of metal atoms. Indeed each of the center atoms, Au11, Au13, and Au11′, has six M–M–M bond angles (M = Au, Ag) close to linearity (>170°). For example, Au13–Au11–Ag11 is

(13) Teo, B. K.; Keating, K. *J. Am. Chem. Soc.* **1984**, *106*, 2224.

Table II. Atomic Positional Parameters and Equivalent Isotropic Displacement Parameters and Their Estimated Standard Deviations for Cluster $[(p\text{-Tol}_3P)_{10}Au_{13}Ag_{12}Br_8](PF_6)\cdot 10EtOH$ (**1**)

Atom	x	y	z	B,[a] Å^2	Atom	x	y	z	B,[a] Å^2
Au1	0.1575 (1)	0.0903 (1)	0.8001 (1)	2.82 (5)	C2C6	−0.174 (4)	0.441 (3)	0.810 (3)	4 (1)*
Au2	−0.0036 (1)	0.2236 (1)	0.8387 (1)	3.02 (5)	C2A7	0.336 (6)	0.437 (6)	0.638 (5)	7 (3)*
Au3	−0.1514 (1)	0.1598 (1)	0.8578 (1)	2.99 (5)	C2C7	−0.277 (6)	0.583 (6)	0.673 (5)	6 (3)*
Au4	−0.0780 (1)	0.0001 (1)	0.8099 (1)	2.87 (5)	C2B7	−0.123 (7)	0.514 (6)	1.067 (6)	10 (3)*
Au5	0.1093 (1)	−0.0490 (1)	0.7898 (1)	2.85 (5)	C3A1	−0.314 (3)	0.322 (3)	0.910 (3)	3 (1)*
Au11	0.0039 (1)	0.0623 (1)	0.86940 (9)	1.97 (4)	C3B1	−0.378 (3)	0.192 (3)	0.889 (3)	3 (1)*
Au13	0.000	0.000	1.000	7.0 (1)	C3C1	−0.292 (4)	0.298 (4)	0.782 (3)	5 (1)*
Ag1	0.1554 (2)	−0.0468 (3)	0.9042 (2)	3.3 (1)	C3A2	−0.291 (4)	0.309 (4)	0.960 (3)	5 (1)*
Ag2	0.0918 (2)	0.1194 (3)	0.9341 (2)	3.4 (1)	C3B2	−0.421 (6)	0.205 (6)	0.939 (5)	9 (3)*
Ag3	−0.0921 (3)	0.1613 (3)	0.9675 (2)	3.3 (1)	C3C2	−0.217 (4)	0.306 (4)	0.730 (3)	4 (1)*
Ag4	−0.1483 (2)	0.0203 (3)	0.9523 (2)	3.3 (1)	C3C3	−0.223 (5)	0.346 (5)	0.678 (5)	8 (2)*
Ag5	−0.0002 (3)	−0.1040 (2)	0.9119 (2)	3.3 (1)	C3B3	−0.503 (5)	0.165 (5)	0.968 (4)	8 (2)*
Ag11	0.0104 (3)	0.1239 (3)	0.7426 (2)	3.2 (1)	C3A3	−0.304 (6)	0.360 (5)	1.014 (5)	8 (2)*
Br1	0.1419 (4)	−0.2240 (4)	0.9257 (3)	3.9 (1)	C3B4	−0.508 (4)	0.120 (4)	0.927 (3)	4 (1)*
Br2	0.2838 (3)	−0.0646 (4)	0.9536 (3)	4.6 (2)	C3A4	−0.358 (4)	0.444 (4)	0.993 (3)	5 (1)*
Br3	−0.1346 (4)	−0.1695 (4)	0.9810 (3)	4.9 (2)	C3C4	−0.297 (5)	0.378 (5)	0.655 (4)	7 (2)*
Br11	0.0108 (5)	0.1862 (6)	0.6291 (4)	7.9 (3)	C3B5	−0.442 (4)	0.100 (4)	0.884 (4)	6 (2)*
P1	0.2887 (8)	0.1156 (9)	0.7454 (8)	3.5 (4)	C3C5	−0.372 (5)	0.372 (5)	0.695 (4)	7 (2)*
P2	−0.0111 (8)	0.3609 (8)	0.8166 (8)	3.5 (4)	C3A5	−0.383 (5)	0.455 (5)	0.938 (4)	7 (2)*
P3	−0.2859 (9)	0.2445 (9)	0.8591 (9)	3.9 (4)	C3B6	−0.375 (5)	0.139 (5)	0.860 (4)	7 (2)*
P4	−0.1423 (9)	−0.044 (1)	0.7478 (8)	3.7 (4)	C3A6	−0.376 (4)	0.397 (4)	0.900 (3)	5 (1)*
P5	0.2085 (8)	−0.1475 (9)	0.7298 (8)	3.4 (4)	C3C6	−0.368 (4)	0.336 (4)	0.759 (3)	5 (1)*
P6	0.529 (2)	0.395 (2)	0.443 (2)	2.7 (7)	C3B7	−0.572 (5)	0.071 (4)	0.954 (4)	6 (2)*
F1	0.398 (7)	0.620 (7)	0.607 (6)	10 (4)	C3C7	−0.291 (6)	0.408 (6)	0.592 (5)	9 (3)*
F2	0.435 (6)	0.679 (6)	0.500 (5)	10 (3)	C3A7	−0.372 (5)	0.511 (5)	1.033 (4)	7 (2)*
F3	0.455 (7)	0.409 (7)	0.485 (6)	12 (4)	C4A1	−0.226 (4)	0.028 (4)	0.722 (3)	4 (1)*
F4	0.508 (7)	0.470 (7)	0.391 (6)	12 (4)	C4B1	−0.074 (4)	−0.076 (4)	0.675 (3)	5 (1)*
F5	0.504 (6)	0.345 (6)	0.424 (5)	10 (3)	C4C1	−0.187 (3)	−0.129 (3)	0.789 (3)	4 (1)*
F6	0.557 (6)	0.458 (6)	0.464 (5)	10 (3)	C4A2	−0.210 (3)	0.108 (3)	0.692 (3)	4 (1)*
C1C1	0.315 (3)	0.185 (3)	0.782 (2)	1.9 (8)*	C4B2	0.009 (3)	−0.065 (3)	0.653 (3)	3 (1)*
C1A1	0.381 (3)	0.026 (3)	0.741 (2)	3 (1)*	C4C2	−0.159 (5)	−0.206 (5)	0.773 (4)	7 (2)*
C1B1	0.298 (3)	0.159 (3)	0.661 (2)	3 (1)*	C4A3	−0.269 (4)	0.163 (4)	0.660 (3)	4 (1)*
C1A2	0.415 (4)	−0.001 (4)	0.789 (4)	6 (2)*	C4B3	0.067 (5)	−0.083 (5)	0.583 (4)	7 (2)*
C1C2	0.392 (6)	0.203 (5)	0.755 (5)	9 (2)*	C4C3	−0.199 (4)	−0.263 (4)	0.804 (4)	6 (2)*
C1B2	0.221 (3)	0.178 (3)	0.635 (3)	4 (1)*	C4B4	0.050 (6)	−0.115 (6)	0.540 (5)	10 (3)*
C1B3	0.233 (5)	0.207 (5)	0.576 (4)	6 (2)*	C4C4	−0.254 (4)	−0.256 (4)	0.855 (4)	6 (2)*
C1A3	0.494 (4)	−0.067 (4)	0.787 (3)	5 (2)*	C4A4	−0.346 (5)	0.141 (4)	0.655 (4)	6 (2)*
C1C3	0.411 (6)	0.256 (6)	0.795 (5)	9 (3)*	C4C5	−0.281 (5)	−0.184 (5)	0.889 (4)	7 (2)*
C1A4	0.519 (3)	−0.103 (3)	0.731 (3)	4 (1)*	C4B5	−0.057 (6)	−0.120 (6)	0.568 (5)	9 (3)*
C1B4	0.313 (6)	0.224 (6)	0.526 (5)	9 (3)*	C4A5	−0.363 (4)	0.076 (4)	0.688 (3)	5 (2)*
C1C4	0.349 (6)	0.294 (6)	0.842 (5)	9 (3)*	C4C6	−0.241 (6)	−0.122 (5)	0.852 (5)	8 (2)*
C1A5	0.483 (4)	−0.083 (4)	0.685 (3)	4 (1)*	C4B6	−0.103 (5)	−0.093 (5)	0.626 (4)	7 (2)*
C1B5	0.376 (5)	0.213 (5)	0.561 (4)	7 (2)*	C4A6	−0.305 (4)	0.019 (4)	0.715 (3)	5 (1)*
C1C5	0.263 (7)	0.277 (6)	0.858 (5)	10 (3)*	C4A7	−0.400 (4)	0.200 (4)	0.627 (4)	6 (2)*
C1A6	0.410 (3)	−0.014 (3)	0.690 (2)	3 (1)*	C4C7	−0.298 (5)	−0.329 (5)	0.888 (4)	7 (2)*
C1B6	0.376 (4)	0.171 (4)	0.621 (3)	4 (1)*	C4B7	0.097 (6)	−0.132 (6)	0.473 (5)	10 (3)*
C1C6	0.253 (4)	0.225 (4)	0.826 (3)	5 (2)*	C5C1	0.257 (4)	−0.105 (4)	0.655 (3)	5 (1)*
C1A7	0.606 (5)	−0.183 (5)	0.726 (4)	7 (2)*	C5A1	0.157 (4)	−0.215 (4)	0.713 (3)	5 (1)*
C1B7	0.312 (6)	0.275 (5)	0.462 (5)	8 (2)*	C5B1	0.293 (5)	−0.215 (5)	0.764 (4)	7 (2)*
C1C7	0.371 (6)	0.353 (5)	0.878 (5)	8 (2)*	C5C2	0.217 (4)	−0.028 (4)	0.627 (3)	5 (2)*
C2A1	0.094 (3)	0.381 (3)	0.765 (2)	3 (1)*	C5A2	0.180 (5)	−0.242 (5)	0.658 (4)	7 (2)*
C2C1	−0.091 (3)	0.428 (3)	0.771 (2)	3 (1)*	C5B2	0.327 (5)	−0.296 (5)	0.747 (4)	7 (2)*
C2B1	−0.044 (4)	0.410 (4)	0.888 (3)	5 (2)*	C5C3	0.253 (4)	0.003 (4)	0.559 (3)	5 (2)*
C2A2	0.115 (6)	0.442 (6)	0.786 (5)	9 (3)*	C5A3	0.134 (6)	−0.306 (6)	0.644 (5)	10 (3)*
C2B2	−0.078 (6)	0.497 (5)	0.881 (5)	8 (2)*	C5B3	0.393 (5)	−0.338 (5)	0.788 (4)	8 (2)*
C2C2	−0.065 (4)	0.454 (4)	0.712 (3)	5 (1)*	C5B4	0.420 (5)	−0.310 (5)	0.832 (4)	7 (2)*
C2A3	0.196 (6)	0.455 (5)	0.744 (5)	8 (2)*	C5A4	0.081 (5)	−0.323 (5)	0.698 (4)	7 (2)*
C2B3	−0.095 (6)	0.534 (6)	0.940 (5)	8 (3)*	C5C4	0.345 (5)	−0.041 (4)	0.528 (4)	6 (2)*
C2C3	−0.133 (5)	0.510 (5)	0.676 (4)	7 (2)*	C5B5	0.394 (5)	−0.222 (5)	0.832 (4)	7 (2)*
C2A4	0.238 (5)	0.425 (5)	0.684 (4)	7 (2)*	C5C5	0.388 (5)	−0.112 (5)	0.564 (4)	7 (2)*
C2B4	−0.103 (6)	0.487 (6)	0.991 (5)	9 (3)*	C5A5	0.060 (4)	−0.302 (4)	0.751 (4)	6 (2)*
C2C4	−0.208 (5)	0.527 (5)	0.707 (4)	7 (2)*	C5B6	0.326 (4)	−0.176 (4)	0.800 (3)	5 (1)*
C2A5	0.210 (6)	0.371 (6)	0.666 (5)	9 (3)*	C5C6	0.347 (4)	−0.148 (4)	0.614 (3)	5 (2)*
C2B5	−0.065 (6)	0.406 (6)	1.006 (5)	7 (3)*	C5A6	0.099 (4)	−0.242 (4)	0.768 (3)	5 (1)*
C2C5	−0.234 (5)	0.500 (5)	0.777 (4)	6 (2)*	C5C7	0.390 (5)	0.003 (5)	0.461 (4)	7 (2)*
C2A6	0.132 (5)	0.348 (5)	0.713 (4)	8 (2)*	C5A7	0.037 (6)	−0.385 (6)	0.689 (5)	10 (3)*
C2B6	−0.029 (5)	0.366 (5)	0.941 (4)	7 (2)*	C5B7	0.492 (6)	−0.357 (6)	0.852 (5)	9 (3)*

[a] Starred B values are for atoms refined isotropically. B values for anisotropically refined atoms are given in the form of the isotropic equivalent displacement parameter defined as $(4/3)[a^2B(1,1) + b^2B(2,2) + c^2B(3,3) + ab(\cos\gamma)B(1,2) + ac(\cos\beta)B(1,3) + bc(\cos\alpha)B(2,3)]$.

178.8 (2)°, Au3–Au11–Ag1 is 170.5 (1)°, and Au1–Au11–Ag4 is 173.7 (1)°, and so on (cf. Table IV).

By definition, an icosahedron has 20 equilateral triangular faces on the surface. In addition, there are 12 pentagonal cross sections, which correspond to dissecting the icosahedron normal to the six 5-fold symmetry axes. Therefore, the peripheral M–M–M angles should be either 60° (triangular face) or 108° (pentagonal cross section). Indeed, Table IV shows that all peripheral M–M–M (M = Au, Ag) angles fall either in the range of 56.1–64.4° or in the range of 102.2–111.7°.

Table III. Selected Interatomic Distances (Å) and Their Estimated Standard Deviations for Cluster $[(p\text{-Tol}_3P)_{10}Au_{13}Ag_{12}Br_8](PF_6)\cdot 10EtOH$ (**1**)[a]

Au1–Au2	3.014 (2)	Au13–Ag4	2.904 (5)
Au1–Au5	2.858 (4)	Au13–Ag5	2.901 (5)
Au1–Au11	2.722 (3)	Ag1–Ag2	2.900 (6)
Au1–Ag1	2.943 (5)	Ag1–Ag5	3.044 (7)
Au1–Ag2	2.888 (5)	Ag1–Ag3′	3.189 (4)
Au1–Ag11	2.975 (5)	Ag1–Ag4′	3.216 (6)
Au1–P1	2.31 (1)	Ag1–Br1	3.097 (8)
Au2–Au3	2.930 (3)	Ag1–Br2	2.622 (9)
Au2–Au11	2.726 (3)	Ag2–Ag3	2.872 (6)
Au2–Ag2	2.992 (5)	Ag2–Ag4′	3.241 (6)
Au2–Ag3	2.920 (4)	Ag2–Ag5′	3.236 (8)
Au2–Ag11	2.900 (6)	Ag2–Br3	2.563 (6)
Au2–P2	2.31 (1)	Ag3–Ag4	3.003 (7)
Au3–Au4	2.944 (3)	Ag3–Ag5′	3.290 (8)
Au3–Au11	2.715 (3)	Ag4–Ag5	2.807 (5)
Au3–Ag3	2.872 (6)	Ag5–Br1	2.716 (7)
Au3–Ag4	2.847 (5)	Ag11–Br11	2.491 (9)
Au3–Ag11	3.107 (4)	Br1–Ag1	3.097 (8)
Au3–P3	2.30 (1)	Br1–Ag3′	2.571 (4)
Au4–Au5	2.945 (3)	Br1–Ag5	2.716 (7)
Au4–Au11	2.719 (4)	Br2–Ag1	2.622 (9)
Au4–Ag4	3.025 (5)	Br2–Ag4′	2.604 (6)
Au4–Ag5	2.941 (5)	Br3–Ag2	2.563 (6)
Au4–Ag11	2.902 (5)	Br3–Ag4′	3.184 (3)
Au4–P4	2.33 (2)	Br3–Ag5′	2.752 (4)
Au5–Au11	2.711 (3)	P1–C1C1	1.81 (6)
Au5–Ag1	2.845 (6)	P1–C1A1	1.83 (4)
Au5–Ag5	2.918 (4)	P1–C1B1	1.82 (5)
Au5–Ag11	3.104 (4)	P2–C2A1	1.89 (5)
Au5–P5	2.30 (1)	P2–C2C1	1.89 (5)
Au11–Au13	2.824 (2)	P2–C2B1	1.78 (8)
Au11–Ag1	2.898 (4)	P3–C3A1	1.79 (6)
Au11–Ag2	2.825 (6)	P3–C3B1	1.92 (6)
Au11–Ag3	2.808 (5)	P3–C3C1	1.76 (7)
Au11–Ag4	2.874 (4)	P4–C4A1	1.74 (6)
Au11–Ag5	2.872 (5)	P4–C4B1	1.75 (6)
Au11–Ag11	2.738 (5)	P4–C4C1	1.83 (6)
Au13–Ag1	2.832 (4)	P5–C5C1	1.73 (6)
Au13–Ag2	2.869 (4)	P5–C5A1	1.82 (8)
Au13–Ag3	2.831 (4)	P5–C5B1	1.81 (8)

[a] Numbers in parentheses are estimated standard deviations in the least significant digits.

C. Staggered–Staggered–Staggered (sss) Metal Configurations. As stated by us earlier,[13] one description of cluster **1** is to recognize that there is an idealized 5-fold symmetry axis passing through atoms Ag11, Au11, Au13, Au11′, and Ag11′ such that the cluster can be viewed as having a metal arrangement of 1:5:1:5:1:5:1:5:1. In this respect, cluster **1** is related to $[Au_{13}(PMe_2Ph)_{10}Cl_2]^{3+}$ [2] and $[Pt_{19}(CO)_{22}]^{4-}$ [3] as depicted schematically in Figure 1 of ref 10c. Here the Au_{13} cluster has a metal arrangement of 1:5:1:5:1 whereas the Pt_{19} cluster has a metal disposition of 1:5:1:5:1:5:1. Furthermore, the adjacent metal pentagons in the cationic Au_{13} and $Au_{13}Ag_{12}$ clusters are staggered (designated as s) with respect to one another, giving rise to *icosahedral* (or *bicapped pentagonal antiprismatic*) *cages* whereas those in the anionic Pt_{19} cluster are eclipsed (designated as e), giving rise to *bicapped pentagonal prismatic cages*. The metal configurations for the Au_{13}, Pt_{19}, and $Au_{13}Ag_{12}$ clusters can therebore be designated as s, ee, and sss, respectively.

The size of the encapsulated metal atoms may play a role in determining the configuration of the metal framework: a more positively charged encapsulated atom would favor smaller icosahedral cages such as those observed in the gold clusters whereas a more negatively charged encapsulated atom would favor larger bicapped pentagonal prismatic cages such as those observed in the platinum cluster.

The Au and Ag pentagons (which are perpendicular to the idealized 5-fold symmetry axis) are nearly parallel. Least-squares planes, along with the perpendicular distances of some of the atoms, are tabulated in Table E. It can be seen that the interplanar distances are Au pentagon–Au pentagon = 2.476 (1.077 + 1.399) Å and Ag pentagon–Ag pentagon = 2.848 (2 × 1.424) Å. It is interesting to note that Au11 is closer to the Au pentagon (1.077 Å) than to the Ag pentagon (1.399 Å). Both distances are smaller than the corresponding distance of 1.424 Å from Au13 to the two Ag pentagons. This observation supports the description of the structure of the two Au-centered icosahedra sharing one Au vertex (vide supra).

D. Ligand Environments. Under the $P\bar{1}$ space group, the modes of bonding of the four crystallographically independent bromide ligands are as follows. Br11 is bonded to Ag11 as a terminal ligand with an Ag11–Br11 distance of 2.49 Å. Br2 is a symmetric double bridge: Br2–Ag1 = 2.62 Å; Br2–Ag4′ = 2.60 Å, and Ag1–Br2–Ag4′ = 75.9°. Br1 is an asymmetric triple bridge: Br1–Ag1 = 3.10 Å, Br1–Ag5 = 2.72 Å, Br1–Ag3′ = 2.57 Å, Ag1–Br1–Ag5 = 62.8°, Ag1–Br1–Ag3′ = 66.8°, and Ag5–Br1–Ag3′ = 76.0°. Br3 is also an asymmetric triple bridge: Br3–Ag5′ = 2.75 Å, Br3–Ag4′ = 3.18 Å, Br3–Ag2 = 2.56 Å, Ag5′–Br3–Ag4′ = 55.0°, Ag2–Br3–Ag5′ = 74.0°, and Ag4′–Br3–Ag2 = 66.8°. It is interesting to note that the two shorter Br–Ag distances of the asymmetric triple bridges, Br1 and Br3, give rise to average values of 2.65 and 2.66 Å, respectively, which are very close to the average value of 2.61 Å of the symmetric double bridge, Br2. Furthermore, the largest Ag–Br–Ag bridging angle for each of the asymmetric triple bridges, 76.1° for Br1 and 74.0° for Br3 (which subtend the shortest Br–Ag distances), is similar to that of 75.9° for the symmetric double bridge (Br2). In this respect, all six bridging bromine ligands (Br1, Br2, Br3, Br1′, Br2′, Br3′) may also be considered as doubly bridging. This ambiguity will be discussed in detail when we consider electron counting in a later section (section III.J).

The six bridging bromine ligands form an approximate (planar) hexagon with nonbonding Br···Br distances ranging from 4.32 to 4.42 Å; these distances are greater than the sum of van der Waals radii 3.90 Å. The least-squares plane of the Br hexagon is tabulated in Table E. The disposition of the Br hexagon in relation to the two central Ag pentagons, as projected down the idealized 5-fold rotation axis, is depicted in Figure 2. It is evident from this projection that the heavy-atom framework $[P_{10}Au_{13}Ag_{12}Br_8]$ of cluster **1** possesses two additional idealized symmetry elements: a 2-fold rotation axis passing through Au13 and Br2 and a reflection plane passing through Au2, Ag5, Au11, and Au13.

It should be emphasized that the disposition of the six bridging bromine ligands in **1**, with respect to the two pentagonal silver rings, is distinctly different from that observed by Teo and Keating.[13]

The five crystallographically independent tri-*p*-tolylphosphine ligands are coordinated to five peripheral Au atoms (Au1–Au5) in a radial fashion, viz., radiated from the central Au atom, Au11 (cf. Table IV). The Au11–Au*i*–P*i* (*i* = 1–5) angles range from 173.4 to 177.9°. The five Au–P distances fall into a normal range of 2.30–2.36 Å with a mean of 2.31 Å.

E. Anions: Positional Disorder and Orientation Order. The nature and the number of anions in the crystal structure of $[(Ph_3P)_{10}Au_{13}Ag_{12}Br_8](PF_6)\cdot 10EtOH$ (**1**) deserve some comments. In **1**, we found one PF_6^- per asymmetric unit, situated at the general position (0.52, 0.39, 0.44). The centrosymmetric space group $P\bar{1}$ implies the existence of two PF_6^- units per unit cell related by the crystallographic inversion center at ($^1/_2$, $^1/_2$, $^1/_2$). However, a close examination of the van der Waals contacts between the two PF_6^- anions (which are separated by an unusually short distance of 4.59 Å) revealed unusually short intermolecular F···F distances of, e.g., F6···F6′ at 2.40 Å and F6···F3′ at 2.70 Å. These latter distances are 1 Å (or more) shorter than the sum of van der Waals radius of F (3.6 Å). It is, therefore, concluded that the occupancy of the PF_6^- anion should be $^1/_2$ and that there is only one PF_6^- per unit cell. Since there is only one cationic cluster per unit cell, the correct formulation of the crystal structure of **1** should be $[(p\text{-Tol}_3P)_{10}Au_{13}Ag_{12}Br_8](PF_6)$.

Although equally split between the two centrosymmetrically related locations (i.e., 50% occupancy), the individual PF_6^- anion is well-ordered. This is reflected in the isotropic thermal parameters of 2.7 (7) Å^2 for the P atom in the anion, which is reasonable compared with the corresponding values of 3.4–3.9 Å

Table IV. Selected Bond Angles (deg) and Their Estimated Standard Deviations for Cluster $[(p\text{-Tol}_3P)_{10}Au_{13}Ag_{12}Br_8](PF_6)\cdot 10EtOH$

Au2-Au1-Au5	108.18 (9)	Ag4-Au4-Ag5	56.1 (1)	Ag1-Au11-Ag2	60.9 (1)	Au3-Ag3-Au11	57.1 (1)
Au2-Au1-Au11	56.46 (7)	Ag4-Au4-Ag11	110.0 (2)	Ag1-Au11-Ag3	110.1 (2)	Au3-Ag3-Au13	106.6 (2)
Au2-Au1-Ag1	108.3 (1)	Ag4-Au4-P4	125.9 (4)	Ag1-Au11Ag4	110.7 (1)	Au3-Ag3-Ag2	110.3 (2)
Au2-Au1-Ag2	60.9 (1)	Ag5-Au4-Ag11	112.1 (2)	Ag1-Au11-Ag5	63.7 (1)	Au3-Ag3-Ag4	57.9 (1)
Au2-Au1-Ag11	57.9 (1)	Ag5-Au4-P4	124.5 (4)	Ag1-Au11-Ag11	120.0 (1)	Au11-Ag3-Au13	60.09 (9)
Au2-Au1-P1	122.9 (4)	Ag11-Au4-P4	115.2 (4)	Ag2-Au11-Ag3	61.3 (1)	Au11-Ag3-Ag2	59.6 (1)
Au5-Au1-Au11	58.06 (8)	Au1-Au5-Au4	106.78 (8)	Ag2-Au11-Ag4	113.8 (1)	Au11-Ag3-Ag4	59.2 (1)
Au5-Au1-Ag1	58.7 (1)	Au1-Au5-Au11	58.46 (8)	Ag2-Au11-Ag5	113.9 (1)	Au13-Ag3-Ag2	60.4 (1)
Au5-Au1-Ag2	106.9 (1)	Au1-Au5-Ag1	62.1 (1)	Ag2-Au11-Ag11	117.8 (2)	Au13-Ag3-Ag4	59.6 (1)
Au5-Au1-Ag11	64.3 (1)	Au1-Au5-Ag5	111.5 (1)	Ag3-Au11-Ag4	63.8 (1)	Ag2-Ag3-Ag4	108.7 (2)
Au5-Au1-P1	123.8 (4)	Au1-Au5-Ag11	59.7 (1)	Ag3-Au11-Ag5	111.4 (1)	Au3-Ag4-Au4	60.1 (1)
Au11-Au1-Ag1	61.38 (9)	Au1-Au5-P5	119.1 (4)	Ag3-Au11-Ag11	119.6 (1)	Au3-Ag4-Au11	56.67 (9)
Au11-Au1-Ag2	60.4 (1)	Au4-Au5-Au11	57.30 (8)	Ag4-Au11-Ag5	58.5 (1)	Au3-Ag4-Au13	105.3 (2)
Au11-Au1-Ag11	57.25 (9)	Au4-Au5-Ag1	111.4 (1)	Ag4-Au11-Ag11	119.8 (2)	Au3-Ag4-Ag3	58.7 (1)
Au11-Au1-P1	177.3 (5)	Au4-Au5-Ag5	60.2 (1)	Ag5-Au11-Ag11	119.5 (2)	Au3-Ag4-Ag5	110.1 (2)
Ag1-Au1-Ag2	59.6 (1)	Au4-Au5-Ag11	57.3 (1)	Au11-Au13-Ag1	61.6 (1)	Au3-Ag4-Br3	146.5 (2)
Ag1-Au1-Ag11	111.1 (1)	Au4-Au5-P5	128.0 (5)	Au11-Au13-Ag2	59.5 (1)	Au4-Ag4-Au11	54.8 (1)
Ag1-Au1-P1	117.5 (4)	Au11-Au5-Ag1	62.8 (1)	Au11-Au13-Ag3	59.6 (1)	Au4-Ag4-Au13	105.6 (1)
Ag2-Au1-Ag11	108.7 (1)	Au11-Au5-Ag5	61.2 (1)	Au11-Au13-Ag4	60.21 (9)	Au4-Ag4-Ag3	104.9 (2)
Ag2-Au1-P1	117.0 (5)	Au11-Au5-Ag11	55.70 (9)	Au11-Au13-Ag5	60.20 (9)	Au4-Ag4-Ag5	60.4 (1)
Ag11-Au1-P1	125.0 (4)	Au11-Au5-P5	173.7 (5)	Ag1-Au13-Ag2	61.1 (1)	Au4-Ag4-Br3	88.1 (2)
Au1-Au2-Au3	108.4 (1)	Ag1-Au5-Ag5	63.8 (1)	Ag1-Au13-Ag3	111.4 (1)	Au11-Ag4-Au13	58.50 (9)
Au1-Au2-Au11	56.35 (7)	Ag1-Au5-Ag11	110.2 (1)	Ag1-Au13-Ag4	111.7 (1)	Au11-Ag4-Ag3	57.0 (1)
Au1-Au2-Ag2	57.48 (9)	Ag1-Au5-P5	110.8 (5)	Ag1-Au13-Ag5	64.1 (1)	Au11-Ag4-Ag5	60.7 (1)
Au1-Au2-Ag3	104.7 (1)	Ag5-Au5-Ag11	107.1 (1)	Ag2-Au13-Ag3	60.5 (1)	Au11-Ag4-Br3	114.8 (2)
Au1-Au2-Ag11	60.4 (1)	Ag5-Au5-P5	117.1 (4)	Ag2-Au13-Ag4	111.6 (1)	Au13-Ag4-Ag3	57.2 (1)
Au1-Au2-P2	124.5 (3)	Ag11-Au5-P5	129.2 (4)	Ag2-Au13-Ag5	111.7 (1)	Au13-Ag4-Ag5	61.0 (1)
Au3-Au2-Au11	57.25 (7)	Au1-Au11-Au2	67.18 (8)	Ag3-Au13-Ag4	63.1 (1)	Au13-Ag4-Br3	92.3 (2)
Au3-Au2-Ag2	105.5 (1)	Au1-Au11-Au3	124.92 (9)	Ag3-Au13-Ag5	109.8 (1)	Ag3-Ag4-Ag5	107.6 (2)
Au3-Au2-Ag3	58.8 (1)	Au1-Au11-Au4	117.8 (1)	Ag4-Au13-Ag5	57.8 (1)	Ag3-Ag4-Br3	148.9 (2)
Au3-Au2-Ag11	64.4 (1)	Au1-Au11-Au5	63.48 (8)	Au1-Ag1-Au5	59.2 (1)	Ag5-Ag4-Br3	54.3 (2)
Au3-Au2-P2	122.8 (4)	Au1-Au11-Au13	112.88 (9)	Au1-Ag1-Au11	55.56 (9)	Au4-Ag5-Au5	60.3 (1)
Au11-Au2-Ag2	59.0 (1)	Au1-Au11-Ag1	63.1 (1)	Au1-Ag1-Au13	106.3 (1)	Au4-Ag5-Au11	55.8 (1)
Au11-Au2-Ag3	59.5 (1)	Au1-Au11-Ag2	62.7 (1)	Au1-Ag1-Ag2	59.2 (1)	Au4-Ag5-Au13	107.9 (1)
Au11-Au2-Ag11	58.2 (1)	Au1-Au11-Ag3	116.3 (1)	Au1-Ag1-Ag5	105.8 (2)	Au4-Ag5-Ag1	106.0 (2)
Au11-Au2-P2	177.9 (5)	Au1-Au11-Ag4	173.7 (1)	Au1-Ag1-Br1	138.6 (2)	Au4-Ag5-Ag4	63.4 (1)
Ag2-Au2-Ag3	58.1 (1)	Au1-Au11-Ag5	117.2 (1)	Au1-Ag1-Br2	107.6 (2)	Au4-Ag5-Br1	140.3 (2)
Ag2-Au2-Ag11	107.9 (1)	Au1-Au11-Ag11	66.0 (1)	Au5-Ag1-Au11	56.3 (1)	Au4-Ag5-Br3	98.6 (2)
Ag2-Au2-P2	119.5 (5)	Au2-Au11-Au3	65.16 (8)	Au5-Ag1-Au13	106.5 (1)	Au5-Ag5-Au11	55.82 (9)
Ag3-Au2-Ag11	110.9 (2)	Au2-Au11-Au4	117.5 (1)	Au5-Ag1-Ag2	106.9 (2)	Au5-Ag5-Au13	102.8 (2)
Ag3-Au2-P2	118.5 (4)	Au2-Au11-Au5	122.09 (9)	Au5-Ag1-Ag5	59.3 (1)	Au5-Ag5-Ag1	56.9 (1)
Ag11-Au2-P2	123.9 (5)	Au2-Au11-Au13	115.2 (1)	Au5-Ag1-Br1	80.2 (2)	Au5-Ag5-Ag4	110.9 (2)
Au2-Au3-Au4	104.84 (8)	Au2-Au11-Ag1	118.3 (1)	Au5-Ag1-Br2	144.7 (2)	Au5-Ag5-Br1	85.6 (2)
Au2-Au3-Au11	57.59 (7)	Au2-Au11-Ag2	65.2 (1)	Au11-Ag1-Au13	59.03 (8)	Au5-Ag5-Br3	151.5 (3)
Au2-Au3-Ag3	60.4 (1)	Au2-Au11-Ag3	63.7 (1)	Au11-Ag1-Ag2	58.3 (1)	Au11-Ag5-Au13	58.6 (1)
Au2-Au3-Ag4	111.4 (1)	Au2-Au11-Ag4	116.9 (1)	Au11-Ag1-Ag5	57.7 (1)	Au11-Ag5-Ag1	58.6 (1)
Au2-Au3-Ag11	57.3 (1)	Au2-Au11-Ag5	174.9 (1)	Au11-Ag1-Br1	109.5 (2)	Au11-Ag5-Ag4	60.8 (1)
Au2-Au3-P3	121.7 (4)	Au2-Au11-Ag11	64.1 (1)	Au11-Ag1-Br2	147.0 (3)	Au11-Ag5-Br1	122.4 (2)
Au4-Au3-Au11	57.26 (8)	Au3-Au11-Au4	65.60 (9)	Au13-Ag1-Ag2	60.1 (1)	Au11-Ag5-Br3	130.5 (2)
Au4-Au3-Ag3	110.5 (1)	Au3-Au11-Au5	125.9 (1)	Au13-Ag1-Ag5	59.0 (1)	Au13-Ag5-Ag1	56.8 (1)
Au4-Au3-Ag4	63.0 (1)	Au3-Au11-Au13	111.25 (7)	Au13-Ag1-Br1	91.7 (2)	Au13-Ag5-Ag4	61.1 (1)
Au4-Au3-Ag11	57.2 (1)	Au3-Au11-Ag1	170.5 (1)	Au13-Ag1-Br2	108.7 (2)	Au13-Ag5-Br1	98.5 (2)
Au4-Au3-P3	126.8 (5)	Au3-Au11-Ag2	116.6 (1)	Ag2-Ag1-Ag5	106.8 (2)	Au13-Ag5-Br3	102.0 (2)
Au11-Au3-Ag3	60.3 (1)	Au3-Au11-Ag3	62.6 (1)	Ag2-Ag1-Br1	151.7 (2)	Ag1-Ag5-Ag4	108.4 (2)
Au11-Au3-Ag4	62.17 (9)	Au3-Au11-Ag4	61.2 (1)	Ag2-Ag1-Br2	88.7 (2)	Ag1-Ag5-Br1	64.8 (2)
Au11-Au3-Ag11	55.62 (9)	Au3-Au11-Ag5	112.1 (1)	Ag5-Ag1-Br1	52.5 (2)	Ag1-Ag5-Br3	151.4 (3)
Au11-Au3-P3	174.0 (5)	Au3-Au11-Ag11	69.5 (1)	Ag5-Ag1-Br2	146.5 (2)	Ag4-Ag5-Br1	155.5 (3)
Ag3-Au3-Ag4	63.4 (1)	Au4-Au11-Au5	65.68 (8)	Br1-Ag1-Br2	101.0 (2)	Ag4-Ag5-Br3	69.9 (2)
Ag3-Au3-Ag11	106.5 (1)	Au4-Au11-Au13	116.86 (8)	Au1-Ag2-Au2	61.6 (1)	Br1-Ag5-Br3	104.4 (2)
Ag3-Au3-P3	113.9 (5)	Au4-Au11-Ag1	116.7 (1)	Au1-Ag2-Au11	56.9 (1)	Au1-Ag11-Au2	61.7 (1)
Ag4-Au3-Ag11	109.2 (1)	Au4-Au11-Ag2	177.3 (1)	Au1-Ag2-Au13	106.8 (2)	Au1-Ag11-Au3	104.9 (1)
Ag4-Au3-P3	114.7 (4)	Au4-Au11-Ag3	119.6 (1)	Au1-Ag2-Ag1	61.1 (1)	Au1-Ag11-Au4	104.8 (1)
Ag11-Au3-P3	129.8 (5)	Au4-Au11-Ag4	65.4 (1)	Au1-Ag2-Ag3	109.3 (2)	Au1-Ag11-Au5	56.0 (1)
Au3-Au4-Au5	110.3 (1)	Au4-Au11-Ag5	63.4 (1)	Au2-Ag2-Au11	55.8 (1)	Au1-Ag11-Au11	56.7 (1)
Au3-Au4-Au11	57.14 (8)	Au4-Au11-Ag11	64.2 (1)	Au2-Ag2-Au13	106.1 (2)	Au1-Ag11-Br11	124.5 (3)
Au3-Au4-Ag4	57.0 (1)	Au5-Au11-Au13	110.54 (8)	Au2-Ag2-Ag1	110.0 (2)	Au2-Ag11-Au3	58.3 (1)
Au3-Au4-Ag5	103.9 (1)	Au5-Au11-Ag1	60.9 (1)	Au2-Ag2-Ag3	59.7 (1)	Au2-Ag11-Au4	106.7 (1)
Au3-Au4-Ag11	64.2 (1)	Au5-Au11-Ag2	113.0 (1)	Au11-Ag2-Au13	59.4 (1)	Au2-Ag11-Au5	104.8 (2)
Au3-Au4-P4	121.6 (3)	Au5-Au11-Ag3	170.5 (1)	Au11-Ag2-Ag1	60.8 (1)	Au2-Ag11-Au11	57.7 (1)
Au5-Au4-Au11	57.02 (8)	Au5-Au11-Ag4	115.3 (1)	Au11-Ag2-Ag3	59.1 (1)	Au2-Ag11-Br11	120.0 (3)
Au5-Au4-Ag4	104.4 (1)	Au5-Au11-Ag5	63.0 (1)	Au13-Ag2-Ag1	58.8 (1)	Au3-Ag11-Au4	58.55 (9)
Au5-Au4-Ag5	59.4 (1)	Au5-Au11-Ag11	69.4 (1)	Au13-Ag2-Ag3	59.1 (1)	Au3-Ag11-Au5	102.2 (1)
Au5-Au4-Ag11	64.1 (1)	Au13-Au11-Ag1	59.33 (9)	Ag1-Ag2-Ag3	108.3 (2)	Au3-Ag11-Au11	54.93 (9)
Au5-Au4-P4	120.9 (3)	Au13-Au11-Ag2	61.06 (9)	Au2-Ag3-Au3	60.8 (1)	Au3-Ag11-Br11	122.6 (2)
Au11-Au4-Ag4	59.8 (1)	Au13-Au11-Ag3	60.36 (9)	Au2-Ag3-Au11	56.79 (9)	Au4-Ag11-Au5	58.61 (9)
Au11-Au4-Ag5	60.8 (1)	Au13-Au11-Ag4	61.3 (1)	Au2-Ag3-Au13	109.1 (1)	Au4-Ag11-Au11	57.6 (1)
Au11-Au4-Ag11	58.2 (1)	Au13-Au11-Ag5	61.2 (1)	Au2-Ag3-Ag2	62.2 (1)	Au4-Ag11-Br11	123.1 (3)
Au11-Au4-P4	173.3 (4)	Au13-Au11-Ag11	178.8 (1)	Au2-Ag3-Ag4	107.3 (2)	Au5-Ag11-Au11	54.86 (9)

Table IV (Continued)

Au5-Ag11-Br11	128.0 (3)	C1A1-P1-C1B1	104 (2)	Au4-P4-C4B1	114 (3)	F1-P6-F4	78 (7)
Au11-Ag11-Br11	177.1 (3)	Au2-P2-C2A1	112 (2)	Au4-P4-C4C1	114 (2)	F1-P6-F5	89 (7)
Ag1-Br1-Ag5	62.8 (2)	Au2-P2-C2C1	118 (2)	C4A1-P4-C4B1	102 (3)	F1-P6-F6	92 (6)
Ag1-Br1-Ag3′	66.8 (2)	Au2-P2-C2B1	113 (2)	C4A1-P4-C4C1	104 (3)	F2-P6-F3	87 (6)
Ag3′-Br1-Ag5	76.0 (3)	C2A1-P2-C2C1	103 (2)	C4B1-P4-C4C1	105 (3)	F2-P6-F4	170 (7)
Ag1-Br2-Ag4′	75.9 (2)	C2A1-P2-C2B1	109 (3)	Au5-P5-C5C1	111 (2)	F2-P6-F5	90 (8)
Ag2-Br3-Ag4′	66.8 (2)	C2C1-P2-C2B1	100 (3)	Au5-P5-C5A1	111 (2)	F2-P6-F6	93 (8)
Ag2-Br3-Ag5′	74.0 (1)	Au3-P3-C3A1	112 (2)	Au5-P5-C5B1	118 (3)	F3-P6-F4	98 (7)
Ag4′-Br3-Ag5′	55.0 (1)	Au3-P3-C3B1	115 (2)	C5C1-P5-C5A1	105 (4)	F3-P6-F5	86 (7)
Au1-P1-C1C1	113 (1)	Au3-P3-C3C1	112 (2)	C5C1-P5-C5B1	107 (3)	F3-P6-F6	93 (7)
Au1-P1-C1A1	115 (2)	C3A1-P3-C3B1	106 (2)	C5A1-P5-C5B1	104 (4)	F4-P6-F5	99 (8)
Au1-P1-C1B1	115 (2)	C3A1-P3-C3C1	104 (3)	F1-P6-F2	97 (6)	F4-P6-F6	78 (8)
C1C1-P1-C1A1	104 (2)	C3B1-P3-C3C1	107 (3)	F1-P6-F3	173 (9)	F5-P6-F6	178 (7)
C1C1-P1-C1B1	105 (2)	Au4-P4-C4A1	116 (3)				

[a] Numbers in parentheses are estimated standard deviations in the least significant digits.

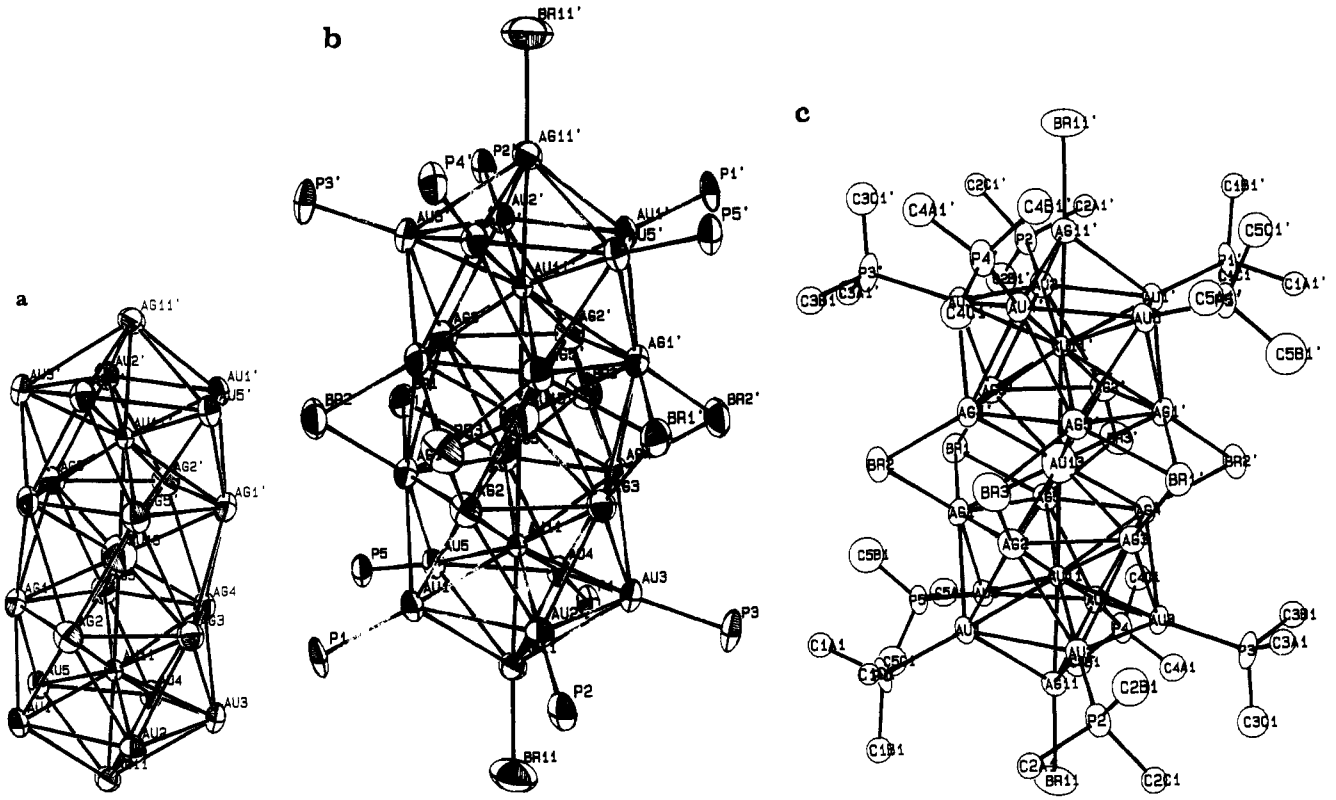

Figure 1. Molecular architecture of the 25-atom cluster $[(p\text{-Tol}_3P)_{10}Au_{13}Ag_{12}Br_8]^+$ as the PF_6^- salt (**1**): (a) metal framework, $Au_{13}Ag_{12}$, only; (b) framework with ligands, $P_{10}Au_{13}Ag_{12}Br_8$; (c) framework with ligands and with α-carbons of the tolyl groups. The cluster **1** conforms to a *crystallographic* inversion symmetry located at Au13. The symmetry-related atoms are designated as primes (some are not labeled for the sake of clarity). The metal framework has an idealized 5-fold rotation symmetry (passing through Ag11, Au11, Au13, Au11′, and Ag11′). Two additional idealized symmetry elements can be identified (see Figure 2): a 2-fold rotation axis (passing through Br2 and Au13) and a (perpendicular) reflection plane (passing through atoms Au2, Ag5, Ag11, Au11, and Au13), giving rise to a *noncrystallographic* site symmetry of $2/m$ (C_{2h}). All bonds (12 each) radiated from the encapsulated atoms, Au11, Au13, and Au11′, have been omitted for clarity.

for the phosphorus atoms of the cationic cluster **1**. The thermal parameters of the fluorine atoms are expectedly somewhat higher (cf. Table II).

It is concluded that the PF_6^- anion in the crystal structure of **1** is *positionally disordered* but *orientationally ordered*. The major reason for the orientation is the formation of strong hydrogen bonding between the F atoms of the anion and the H atoms of the phosphine ligands of the cation, as evidenced by the short F···C contacts listed in Table F. Note that the five shortest distances, such as F1···C5B2 at 3.39 Å, F2···C4A7 at 3.23 Å, F3···C2A7 at 3.39 Å, F4···C2A7 at 3.34 Å, and F6···C2A7 at 3.09 Å, are less than the corresponding sum of van der Waals radii (F, 1.8 Å; CH_3, 2.0 Å). This suggests a significant degree of "ion pairing".

F. Disordered Solvent Molecules. Under the space group $P\bar{1}$, 15 crystallographically independent solvent atoms with electron densities greater than 1 e/Å^3 were found in difference Fourier maps. (The "ghost peaks" located in the vicinity of the heavy atoms were disregarded). In some cases, solvents are associated by hydrogen bonding or weak O–H···Br (or C–H···Br) or weak O–H···C_{ring} (or C–H···C_{ring}) interactions with cluster **1**. Interatomic distances shorter than normal van der Waals contacts of cluster **1** and solvents (O–H···Br or C–H···Br distances between 2.7 and 3.8 Å and O–H···C_{ring} or C–H···C_{ring} distances between 2.6 and 3.4 Å) are summarized in Table F. However, not all of these solvent molecules are of unit weight. Some are lost during data collection; some are smeared out due to disorder and/or liquidlike arrangement. As described in the Experimental Section, such disorder was modeled by first refining the occupancy of the solvent atoms with a fixed isotropic temperature factor of 8 Å^2 (roughly the average of the phenyl carbons), followed by refining the isotropic thermal parameter while holding the occupancy fixed. The sum of the occupancies (weight) gives a total of 10.5 solvent atoms per asymmetric unit. Since all solvent atoms were refined as carbon atoms, the latter number should be divided by 1.11 to correct for the fact that one out of three solvent atoms is an oxygen

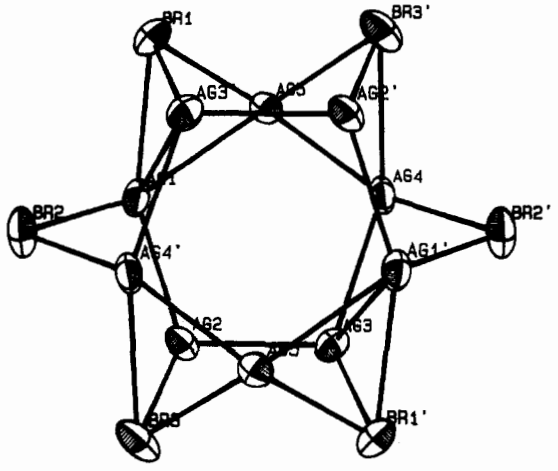

Figure 2. Two staggered Ag_5 (bonding) pentagonal rings linked by a Br_6 (nonbonding) hexagonal ring in the 25-atom cluster $[(p\text{-}Tol_3P)_{10}Au_{13}Ag_{12}Br_8]^+$, as viewed along the idealized 5-fold rotation axis (cf. Figure 1 caption).

atom. The corrected number of solvent atoms is 9.5, or equivalently, 3.15 ethanol molecules per asymmetric unit. Therefore, there are approximately 6.3 ethanol molecules per unit cell. It should be cautioned, however, that the value of 6.3 ethanol molecules per unit cell represents the lower limit, since part of the solvent molecules were lost during data collection. A more realistic number is 10 ethanol molecules per unit cell if we assume full occupancy for each of the 15 solvent atom (15/3 = 5 EtOH per asymmetric unit or 2 × 5 = 10 EtOH per unit cell). Since there is only one monocationic cluster **1** and one PF_6^- anion per unit cell, the overall formula for the crystal should be $[(p\text{-}Tol_3P)_{10}Au_{13}Ag_{12}Br_8](PF_6)\cdot 10EtOH$.

The solvent atoms, and their symmetry-related counterparts, form a network centering at the crystallographic face center (0, $^1/_2$, $^1/_2$). Owing to the disordered nature of the solvent molecules, no attempts were made to interpret their bond lengths and angles. Nonetheless, reasonable bond lengths and angles for CH_3CH_2OH can be identified from the solvent network: e.g., C3–C1–C9, C6–C1–C15, C1–C3–C4, C8–C4–C14, C14–C4–C15, C1–C6–C12, C1–C6–C13, C1–C8–C4, C3–C8–C9, C9–C8–C15, C7–C12–C13, C4–C14–C13, etc.

G. Why Is the Cluster Ordered? It is interesting to ask why the cluster is ordered, given the fact that Au and Ag are roughly equal in size and completely miscible (and randomly distributed) in the alloy solid solution.

We believe the answer lies in the fact that, though both types of ligands coordinate reasonably well with both metals, there is a preference for the halide ligands to bind to the Ag atoms and for the phosphine ligands to bind to the Au atoms. One reason (perhaps not the only reason) is that Ag is more electropositive than Au in the electrochemical series. As a result, the Ag atoms are more positively charged than the Au atoms, as manifested in the trend of metal–metal distances: Au–Au < Au–Ag < Ag–Ag.

In this context, it is interesting to note that the isotropic thermal parameters of all the metal atoms are quite reasonable (B = 2–3 Å^2). The only possible exception is the shared vertex Au13, which has a B value of 7.0 (1) Å^2. This latter value may signify (1) a greater thermal motion (or static disorder) of the gold atom or (2) an admixture of gold and silver atoms at the position of Au13. We prefer the former interpretation, since the shared vertices in all structurally determined Au–Ag supraclusters (characterized by us so far) based on vertex-sharing icosahedra are gold atoms, though the latter possibility cannot be ruled out.

H. Crystal Structure. The crystal structure of the title compound is composed of (1) one discrete cluster **1** located at origin (0, 0, 0), (2) one disordered anion distributed equally at two locations near ($^1/_2$, $^1/_2$, $^1/_2$), and (3) approximately 10 ethanol molecules clustered around (0, $^1/_2$, $^1/_2$), per unit cell. The asymmetric unit comprises half of the above (since the space group is $P\bar{1}$).

Qualitatively, the crystal structure can be described as having the cationic clusters **1** at the corners, the disordered PF_6^- anions near the body center, and solvent molecules clustered around one of the face centers (the *bc* plane) of the triclinic cell.

The cationic cluster, the anion, and the solvent molecules are separated by van der Waals distances. "Intramolecular" and "intermolecular" close van der Waals contacts are tabulated in Table F. Distances shorter than sum of van der Waals radii (Br···CH_3 = 3.95 Å; F···CH_3 = 3.35 Å; CH_3···CH_3 = 4.0 Å) may represent significant hydrogen bonding and/or ion pairing.

The cluster **1** conforms to the crystallographically imposed $\bar{1}$ (C_i) site symmetry. Two idealized symmetry elements can also be identified (cf. Figure 2): a 2-fold rotation axis (passing through Br2 and Au13) and a (perpendicular) reflection plane (passing through atoms Au2, Ag5, Ag11, Au11, and Au13) giving rise to a noncrystallographic symmetry of $2/m$ (C_{2h}). The idealized 2-fold rotation axis is nearly parallel to the crystallographic *a* axis whereas the idealized reflection plane is approximately parallel to the crystallographic *bc* plane. In addition, the metal framework has an idealized 5-fold rotation symmetry (passing through Ag11, Au11, and Au13), which lies approximately in the *bc* plane.

Attempts to refine the structure in space group $P1$ were unsuccessful (viz., resulting in unreasonable parameters). Judging from the ordered nature of the cationic cluster and the reasonable thermal parameters for all the atoms within the cluster, we believe $P\bar{1}$ is the correct space group (at least as far as the cationic cluster is concerned). We cannot, however, rule out the possibility of a $P1$ space group with regard to the anion and/or the solvents (which are highly disordered).

I. Atom Counting. We recently put forth a simple atom counting scheme for supraclusters based on vertex-sharing centered icosahedra.[11] The title cluster **1** is best considered as two 13-atom icosahedra sharing a common vertex in a linear manner. Hence, the nuclearity should be 2 × 13 − 1 = 25 as observed.

As mentioned in ref 11a, the nuclearities (G_n) for three, four, five, seven, and twelve vertex-sharing icosahedra are 36, 46, 56, 75,[11] and 127, respectively. It should be noted that, while the first three members (n = 3–5) of the series follow the general rule $G_n = 10n + 6$, the latter two (n = 7, 12) do not. For n = 7, G_n = 10 × 7 + 6 − 1 = 75 (with one shared atom at the center)[11c] and for n = 12, G_{12} = 10 × 12 + 6 + 1 = 127 (withone additional atom at the center).

Since eqs 6–10 in ref 11a are based on Euler's theorem for superdeltahedra, they also hold for a capped superpolyhedron (viz., further capping of the triangular faces of the superpolyhedron), giving rise to increments of 10, 9, 4, 58, and 116 per capping for G, S, B, T, and N, respectively. For example, bi-, tri-, and tetracapped supertetrahedron will give rise to supraclusters s_6*, s_7*, and s_8* of nuclearities $G_n = 10n + 6$ = 66, 76, and 86, respectively. Thus, though a superoctahedral cluster s_6 is not allowed by symmetry, a super-bicapped-tetrahedral cluster s_6* is stereochemically allowed and is predicted to have a nuclearity of 66.[14] Similarly, while a superhexahedral (viz., supercubic) cluster s_8 is stereochemically rather unlikely, a super-tetracapped-tetrahedral cluster s_8*, with a nuclearity of 86, may well exist.

J. Electron Counting. We recently put forth a cluster of clusters (C^2) model for the electron counting of supraclusters based on vertex-, edge-, or face-sharing of smaller cluster units as building blocks.[11]

With the C^2 approach, the number of skeletal electron pairs for the 25-atom cluster mainframe is B = 2 × 13 (two icosahedra) − 1 × 3 (sharing vertex) = 23. With the topological electron counting (TEC) rule,[15] the total number of electron pairs is $T = 6V_m + B = 6 \times 23 + 23 = 161$. Here V_m is the number of vertices of the cluster, including the shared vertex. Thus, the predicted

(14) After submission of this paper, an alternative s_6' structure based on an edge-sharing bitetrahedral array of six icosahedra has been suggested by Fackler and co-workers (*J. Am. Chem. Soc.* **1989**, *11*, 6434) for a proposed "$(Ph_3P)_{14}Au_{67}Cl_8$" cluster. Stereochemical considerations, however, revealed that the latter structure is unlikely to occur without severe distortions.

(15) Teo, B. K.; Longoni, G.; Chung, F. R. K. *Inorg. Chem.* **1984**, *23*, 1257.

electron count is $N = 2T = 2 \times 161 = 322$. This is in agreement with the observed electron count of $N_{obs} = 10 \times 2$ (phosphine) $+ 25 \times 11$ (metal) $+ 2 \times 1$ (terminal Br) $+ 2 \times 3$ (doubly bridging Br) $+ 4 \times 5$ (triply bridging Br) $- 1$ (monocation) $= 322$.

While the agreement between theory and experiment is pleasingly good, it should be pointed out that the four triply bridging bromine ligands are highly asymmetric (see section III.D for a detailed discussion) and hence can also be considered as doubly bridging. The observed electron count for such a description (viz., with six doubly bridging and two terminal Br ligands) will become $N_{obs} = 322 - 4 \times 2 = 314$. This latter value is 8 electrons below that predicted by the C^2 model, but in good agreement with the shell model[16] of $N = 2T = 2(6G + K) = 2(6 \times 25 + 7) = 2 \times 157 = 314$, where G is the total number of atoms and K is the related to the B value of the "center" of the cluster.

We conclude that the "true" electron count for cluster **1** may lie somewhere between 314 and 322, with the former value representing a cluster with six doubly bridging halogens and the latter value corresponding to a cluster with two doubly bridging and four triply bridging halogen ligands. It should be emphasized, however, that the shell model, which is valid only for close-packed clusters, tends to give lower electron counts than the C^2 model.

Acknowledgment is made to the National Science Foundation (Grant CHE-8722339) and the donors of the Petroleum Research Fund, administered by the American Chemical Society, for financial support of this research. We are also grateful to the University of Illinois at Chicago for a Campus Research Board Award.

Supplementary Material Available: For $[(p\text{-}Tol_3P)_{10}Au_{13}Ag_{12}Br_8](PF_6)\cdot 10EtOH$, full listing of anisotropic thermal parameters (Table A), positional and thermal parameters with the refined occupancy factors for solvent atoms (Table B), interatomic distances (Table C), bond angles (Table D), least-squares planes (Table E), and intra- and intermolecular interactions (Table F) (29 pages); a listing of observed and calculated structure factors (Table G) (98 pages). Ordering information is given on any current masthead page.

(16) Teo, B. K.; Sloane, N. J. A. *Inorg. Chem.* **1985**, *24*, 4545.

Contribution from the Laboratorio di Chimica Inorganica e Nucleare, Dipartimento di Chimica, Università di Ferrara, 44100 Ferrara, Italy, Dipartimento di Chimica Fisica ed Inorganica, Università di Bologna, 40136 Bologna, Italy, and Centro di Strutturistica Diffrattometrica, Dipartimento di Chimica, Università di Ferrara, 44100 Ferrara, Italy

Synthesis of Technetium(V)–Nitrido Complexes with Chelating Amines: A Novel Class of Monocationic, Octahedral Complexes Containing the $[Tc{\equiv}N]^{2+}$ Core. Crystal Structures of $[TcN(en)_2Cl]^+$ (en = Ethylenediamine) and $[TcN(tad)Cl]^+$ (tad = 1,5,8,12-Tetraazadodecane)

Andrea Marchi,*[1] Patrizia Garuti,[1] Adriano Duatti,*[2] Luciano Magon,[1] Roberto Rossi,[1] Valeria Ferretti,[3] and Valerio Bertolasi[3]

Received December 2, 1988

A novel class of monocationic complexes containing the $[Tc{\equiv}N]^{2+}$ functional moiety is reported. The complexes are prepared by substitution reactions on the starting compound $TcNCl_2(PPh_3)_2$ with neutral, bidentate, and tetradentate chelating amines or by reduction with KBH_4 of the complex $[TcNCl_4]^-$ in the presence of the same ligands. The complexes have been characterized by elemental analyses, IR and ^1H NMR spectroscopy, conductivity, and magnetic susceptibility measurements. All the complexes possess a distorted octahedral geometry and, thus, constitute the first homogeneous class of stable, octahedral technetium(V)–nitrido complexes having a sixth, charged ligand in a position trans to the Tc≡N multiple bond. The crystal structures of two members of this class, namely the complexes $[TcN(en)_2Cl]^+$ (**1**) (en = ethylenediamine) and $[TcN(tad)Cl]^+$ (**2**) (tad = 1,5,8,12-tetraazadodecane), have been determined. The complexes have a distorted octahedral structure, with a Cl^- atom in a position trans to the Tc≡N group and two bidentate en ligands in **1** or one tetradentate tad ligand in **2** in the plane normal to the N≡Tc—Cl axis. Compound **1** crystallizes in the space group $P2_1/n$, with $a = 9.316$ (1) Å, $b = 12.404$ (1) Å, $c = 24.367$ (5) Å, $\beta = 93.76$ (1)°, and $V = 2809.7$ (7) Å^3 with $Z = 4$, for 4565 observed reflections with $I \geq 3\sigma(I)$; the Tc≡N bond length is 1.603 (3) Å, while the length of the Tc—Cl bond trans to Tc≡N is 2.7320 (8) Å, which is the longest Tc—Cl bond distance ever observed in technetium chemistry. Compound **2** crystallizes in space group $Pna2_1$ with $a = 9.966$ (2) Å, $b = 31.203$ (10) Å, $c = 9.706$ (4) Å, and $V = 3018$ (2) Å^3 with $Z = 4$, for 2991 observed reflections with $I \geq 3\sigma(I)$; the Tc≡N bond length is 1.626 (6) Å, while the length of the Tc—Cl bond trans to Tc≡N is 2.663 (2) Å.

Introduction

In recent years, it was suggested by Deutsch that atomic or molecular species carrying a positive charge would have a preferential localization in myocardium tissues.[4] Following this hypothesis, a number of monocationic complexes of ^{99m}Tc have been prepared by different groups, with the aim to obtain a ^{99m}Tc-imaging agent for myocardial perfusion.

Deutsch and co-workers reported Tc^{3+} and Tc^+ complexes of the type $[Tc^{III}(dp)_2Cl_2]^+$ and $[Tc^I(dp)_3]^+$ (dp = bidentate diphosphine),[5] while Tc^+ complexes with substituted isocyanide (RCN), $[Tc(RCN)_6]^+$ were described by Davison and co-workers.[6]

(1) Laboratorio di Chimica Inorganica e Nucleare, Dipartimento di Chimica, Università di Ferrara.
(2) Università di Bologna.
(3) Centro di Strutturistica Diffrattometrica, Dipartimento di Chimica, Università di Ferrara.
(4) (a) Deutsch, E.; Bushong, W.; Glavan, K. A.; Elder, R. C.; Sodd, V. J.; Scholz, K. L.; Fortman, D. L.; Lukes, S. J. *Science (Washington D.C.)* **1981**, *214*, 85–86. (b) Deutsch, E.; Glavan, K. A.; Sodd, V. J.; Nishiyama, H.; Ferguson, D. L.; Lukes, S. J. *J. Nucl. Med.* **1981**, *22*, 897–907. (c) Deutsch, E.; Glavan, K. A.; Bushong, W.; Sodd, V. J. In *Applications of Nuclear Chemistry and Radiochemistry*; Lambrecht, R., Marcos, N., Eds.; Pergamon Press: New York, 1982; pp 139–151.
(5) (a) Deutsch, E.; Libson, K.; Jurisson, S.; Lindoy, L. F. *Prog. Inorg. Chem.* **1983**, *30*, 75–139. (b) Kirchoff, J. R.; Heineman, W. R.; Deutsch, E. *Inorg. Chem.* **1987**, *26*, 3108–3113. (c) Vanderheyden, J.-L.; Heeg, M. J.; Deutsch, E. *Inorg. Chem.* **1985**, *24*, 1666–1673. (d) Vanderheyden, J.-L.; Ketring, A. R.; Libson, K.; Heeg, M. J.; Roecker, L.; Motz, P.; Whittle, R.; Elder, R. C.; Deutsch, E. *Inorg. Chem.* **1984**, *23*, 3184–3191. (e) Vanderheyden, J.-L.; Libson, K.; Nosco, D. L.; Ketring, A. R.; Deutsch, E. *Int. J. Appl. Radiat. Isot.* **1983**, *34*, 1611–1618. (f) Libson, K.; Barnett, B. L.; Deutsch, E. *Inorg. Chem.* **1983**, *22*, 1695–1704. (g) Hurst, R. W.; Heineman, W. R.; Deutsch, E. *Inorg. Chem.* **1981**, *20*, 3298–3303.

0020-1669/90/1329-2091$02.50/0